

Two-Microelectrode Voltage Clamp of *Xenopus* Oocytes: Voltage Errors and Compensation for Local Current Flow

W. Baumgartner,^{*,#} L. Islas,[§] and F. J. Sigworth[§]

^{*}Institute for Biophysics, University of Linz, A-4040 Linz, Austria; [#]Institute of Anatomy, University of Würzburg, D-97070 Würzburg, Germany; and [§]Department of Cellular and Molecular Physiology, Yale University School of Medicine, New Haven, Connecticut 06520 USA

ABSTRACT Oocytes from *Xenopus laevis* are commonly used as an expression system for ion channel proteins. The most common method for their electrophysiological investigation is the two-microelectrode voltage clamp technique. The quality of voltage clamp recordings obtained with this technique is poor when membrane currents are large and when rapid charging of the membrane is desired. Detailed mathematical modeling of the experimental setup shows that the reasons for this weak performance are the electrical properties of the oocytes and the geometry of the setup. We measured the cytosolic conductivity to be ~ 5 times lower than that of the typical bath solution, and the specific membrane capacitance to be ~ 6 times higher than that of a simple lipid bilayer. The diameter of oocytes is typically ~ 1 mm, whereas the penetration depth of the microelectrodes is limited to ~ 100 μm . This eccentric current injection, in combination with the large time constants caused by the low conductivity and the high capacitance, yields large deviations from isopotentiality that decay slowly with time constants of up to 150 μs . The inhomogeneity of the membrane potential can be greatly reduced by introducing an additional, extracellular current-passing electrode. The geometrical and electrical parameters of the setup are optimized and initial experiments show that this method should allow for faster and more uniform control of membrane potential.

INTRODUCTION

After the key observation that foreign RNA injected into *Xenopus* oocytes can be translated into proteins (Gurdon et al., 1971) and the first use of oocytes for the expression of receptors and ion channels (Gundersen et al., 1983; Mileedi et al., 1983), oocytes from *Xenopus laevis* have become a popular expression system for ion channels, receptors, and transporters. Ion channels expressed in oocytes can be electrophysiologically investigated by the voltage clamp technique (Marmont, 1949; Cole, 1949; Hodgkin et al., 1949). For oocytes the two-microelectrode voltage clamp is the simplest approach for whole-cell recordings (Stühmer and Parekh, 1995). The principle is depicted in Fig. 1 A. The membrane of the oocyte is penetrated by two microelectrodes, one for voltage sensing and one for current injection. The membrane potential as measured by the voltage-sensing electrode is compared with a command voltage, and the difference is brought to zero by a control amplifier. The injected current is monitored to provide a measure of the total membrane current. Two well-known technical difficulties in voltage clamping of *Xenopus* oocytes arise because of the large size of these cells. First, the limited current that can be provided through a microelectrode limits the rate at which the large membrane capacitance can be charged, thereby limiting the voltage clamp speed. Second, high levels of ion channel expression can result in membrane

currents of 100 μA or more. With currents of this magnitude substantial voltage errors arise due to potential drop in the series resistance in the extracellular solution, which is of the order of 100 Ω . These problems have been addressed through the use of high-voltage amplifiers to force large currents through the current-passing microelectrode, and by the use of electronic compensation for series resistance.

This paper considers a third and arguably the most severe problem in voltage control of oocyte membranes, which arises from potential differences within the cell interior. The theory to be shown confirms observations by ourselves and others that recordings of currents larger than ~ 20 μA are likely to be distorted when obtained with the two-microelectrode voltage clamp. Besides examining the problem of large steady-state currents, in this paper we also consider the transient inhomogeneities in membrane potential that occur when the membrane potential is changed rapidly. We discuss ways to alleviate these problems, including a method to improve voltage clamp performance by using a third microelectrode to compensate for local electric fields.

THEORY

As first pointed out by Rall (1953), expansions in spherical harmonics can be used to compute the spatial variation of membrane potential in spherical cells. Several authors have computed the membrane potential in the case of a point source of membrane current (Hellerstein, 1968; Eisenberg and Engel, 1970; Eisenberg and Johnson, 1970; Peskoff et al., 1972). Peskoff and Eisenberg (1975) and Peskoff and Ramirez (1975) have computed the spatial and temporal variation of membrane potential arising from an intracellular point source of current, such as a microelectrode. Here

Received for publication 30 April 1999 and in final form 22 June 1999.

Address reprint requests to Dr. Werner Baumgartner, Institute of Anatomy, University of Würzburg, Koellikerstrasse 6, D-97070 Würzburg, Germany. Tel.: +49-931-31-2384; Fax: +49-931-31-2712; E-mail: werner.baumgartner@mail.uni-wuerzburg.de.

© 1999 by the Biophysical Society

0006-3495/99/10/1980/12 \$2.00

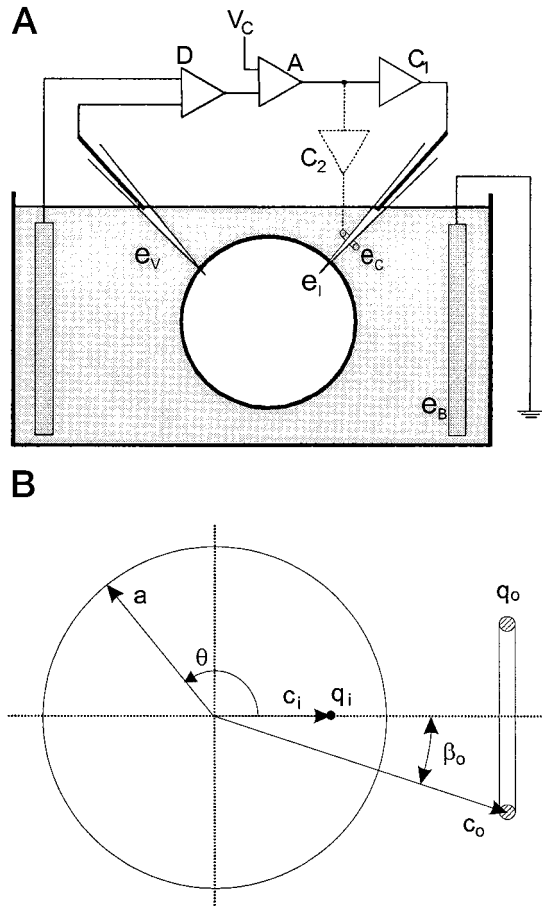


FIGURE 1 The two-microelectrode voltage clamp. (A) Voltage clamp system. A voltage recording electrode e_v monitors membrane potential; this is compared with a command voltage, and the magnified difference is applied to a current injection electrode, e_i . A bath electrode e_b serves as the return path for the injected current. Dashed lines show the proposed modification: the voltage clamp amplifier drives two current sources. One provides current q to the current-injection microelectrode, the other provides a current vq to the extracellular compensation electrode e_c . (B) The geometry of the electrostatic description. Spherical coordinates are used, with r being the distance from the origin, the angle θ defined as shown, and ϕ being the angle about the horizontal axis. Inside the cell, which is a sphere of radius a , is a point source carrying the total current q_i at a distance $r = c_i$ from the center; this represents the current injecting electrode. Outside there is a ring source of current q_o at $r = c_o$ with opening angle β_o representing the compensation electrode. A large, distant bath electrode is assumed, such that the potential $V \rightarrow 0$ as $r \rightarrow \infty$.

we derive expressions for the potential that are equivalent to those of Peskoff and Ramirez (1975) except that we include the effects of an additional extracellular electrode.

General electrostatic description

The geometry of the oocyte voltage clamp is depicted in Fig. 1 B, where the spherical cell membrane of radius a separates the intracellular region having conductivity γ_i from the extracellular region having conductivity γ_o . The potential in this system is obtained by solving the Poisson

equation (Maxwell, 1891)

$$\nabla^2 V = -\frac{\rho}{\epsilon} \quad (1)$$

with V denoting the electric potential, ρ the charge density, and ϵ the dielectric constant. As will be shown later, the conductivities of the media are of the order of 1 S/m. The relaxation time for charge concentration ϵ/γ (Abraham and Becker, 1950) is therefore $<10^{-11}$ s, yielding a quasi-electrostatic description of the field problem appropriate. Instead of charge density ρ we introduce the current source density σ by using the relation

$$\frac{\rho}{\epsilon} = \frac{\sigma}{\gamma} \quad (2)$$

Thus $\rho = 0$ except at the electrodes and directly at the membrane, where the current source density σ is nonzero. As current sources we assume a point source inside the sphere (the current-passing microelectrode tip) with total current q_i , and a ring current source (an extracellular electrode) with total current q_o . To simplify the calculation the Poisson equation is rewritten in spherical coordinates (r, θ, ϕ) yielding

$$\frac{1}{r} \cdot \frac{\partial^2}{\partial r^2} (r \cdot V) + \frac{1}{r^2 \sin \theta} \left(\sin \theta \cdot \frac{\partial V}{\partial \theta} \right) + \frac{1}{r^2 \sin^2 \theta} \cdot \frac{\partial^2 V}{\partial \phi^2} + \frac{\sigma}{\gamma} = 0 \quad (3)$$

The symmetry of the electrode configuration ensures that the potential V will be independent of the azimuthal angle ϕ . We shall solve this equation with inhomogeneous boundary conditions by superimposing the solution of the Poisson equation with homogeneous boundary conditions and the solution of the Laplace equation with inhomogeneous boundary conditions. In our case this Laplace equation is

$$\frac{1}{r} \frac{\partial^2}{\partial r^2} (r \cdot V) + \frac{1}{r^2 \sin \theta} \left(\sin \theta \cdot \frac{\partial V}{\partial \theta} \right) = 0 \quad (4)$$

and has the solution (Jackson, 1962)

$$V = \sum_{l=0}^{\infty} [A_l \cdot r^l + B_l \cdot r^{-(l+1)}] \cdot P_l(\cos \theta) \quad (5)$$

with P_l denoting the Legendre polynomial of the l th order (Abramowitz and Stegun, 1972). The coefficients A_l and B_l are determined from the boundary conditions. To determine these coefficients inside and outside the sphere we use the Dirichlet boundary conditions

$$\begin{array}{ll} \text{inside} & \text{outside} \\ V(r = a, \theta) = V_i(\theta) & V(r = a, \theta) = V_o(\theta) \\ V(r = 0, \theta) < \infty & V(r = \infty, \theta) = 0 \end{array} \quad (6)$$

Here $V_i(\theta)$ and $V_o(\theta)$ denote the membrane potential inside and outside the cell, respectively. These potentials will be determined below. The condition that the electric potential

at $r = \infty$ approaches 0 is actually only an approximation, but it was shown by Peskoff and Ramirez (1975) that the solution of the field problem is almost the same as in the case of a point sink for the current in the vicinity of the cell (the bath electrode) under most experimental conditions. From the above boundary conditions and Eq. 5 one obtains the solution of the Laplace equation (4) inside the sphere to be

$$V = \sum_{l=0}^{\infty} A_l \cdot r^l \cdot P_l(\cos \theta)$$

with

$$\sum_{l=0}^{\infty} A_l \cdot a^l \cdot P_l(\cos \theta) = V_i(\theta) \quad (7)$$

and the solution outside

$$V = \sum_{l=0}^{\infty} B_l \cdot r^{-(l+1)} \cdot P_l(\cos \theta)$$

with

$$\sum_{l=0}^{\infty} B_l \cdot a^{-(l+1)} \cdot P_l(\cos \theta) = V_o(\theta) \quad (8)$$

The next step is to solve the Poisson equation for a ring electrode inside or outside a grounded sphere (i.e., homogeneous boundary conditions). The ring electrode, with angular size β , reduces to a point current source when $\beta = 0$. For a circular source around the symmetry axis consisting of the locus of points (r, θ, ϕ) with $r = c_e$ and $\theta = \beta$, and carrying the total current q , the potential in an infinite medium is (Jackson, 1962)

$$V_{\text{inf}} = \frac{q}{4\pi\gamma} \cdot \sum_{l=0}^{\infty} \frac{r_{<}^l}{r_{>}^{l+1}} \cdot P_l(\cos \beta) \cdot P_l(\cos \theta) \quad (9)$$

with $r_{<}$ ($r_{>}$) denoting the smaller (larger) value of c_e and r . By using this solution one can obtain the potential distribution inside or outside a grounded sphere using the method of images (Jackson, 1962). For this method an imaginary current source corresponding to each original source is placed on the opposite side of the boundary, and the value and position of the image source are adjusted so that the potential at the boundary is the desired value. For the external ring source at radius c_o and with angular extent β_o outside a grounded sphere of radius a , the appropriate image charge is a ring inside the sphere, and vice versa. The solution of the Poisson equation for these two current sources is obtained by superposition using Eq. 9, yielding

$$V = \frac{1}{4\pi\gamma} \cdot \sum_{l=0}^{\infty} \left[q_i \cdot \frac{c_i^l}{r^{l+1}} \cdot P_l(\cos \beta_i) + q_o \cdot \frac{r^l}{c_o} \cdot P_l(\cos \beta_o) \right] \cdot P_l(\cos \theta) \quad (10)$$

with the condition that $V = 0$ at $r = a$. This obviously requires $\beta_i = \beta_o$. Furthermore, as $V(r = a)$ has to be 0 for all values of θ , the following equation must hold for every l :

$$\frac{q_i}{c_i} \cdot \frac{c_i^{l+1}}{a^{l+1}} + \frac{q_o}{a} \cdot \frac{a^{l+1}}{c_o} = 0$$

To fulfill this for every index l the following equations have to hold:

$$\frac{c_i}{a} = \frac{a}{c_o} \quad \text{and} \quad \frac{q_i}{q_o} = -\frac{c_i}{a} \quad (11)$$

Now the media inside and outside the cell have the specific conductivities γ_i and γ_o , respectively. Insertion of Eq. 11 into Eq. 10 yields the solution for a point source inside a grounded sphere carrying the total current q_i to be for $r > c_i$,

$$V = \frac{q_i}{4\pi\gamma_i} \cdot \sum_{l=0}^{\infty} c_i^l \cdot \left(\frac{1}{r^{l+1}} - \frac{r^l}{a^{2l+1}} \right) \cdot P_l(\cos \theta) \quad (12)$$

and for a ring outside carrying the total current q_o for $r < c_o$

$$V = \frac{q_o}{4\pi\gamma_o} \cdot \sum_{l=0}^{\infty} \frac{1}{c_i^{l+1}} \cdot \left(r^l - \frac{a^{2l+1}}{r^{l+1}} \right) \cdot P_l(\cos \beta_o) \cdot P_l(\cos \theta) \quad (13)$$

The potential distribution inside the cell is now obtained by superposition of Eqs. 7 and 12 and outside the cell by superimposing Eqs. 8 and 13. The current density at the interior membrane surface is

$$\begin{aligned} i_i(\theta) &= -\gamma_i \cdot \nabla V|_{r \rightarrow a^+} \\ &= \gamma_i \cdot \sum_{l=0}^{\infty} \left[-A_l \cdot l \cdot a^{l-1} + \frac{q_i}{4\pi\gamma_i} \right. \\ &\quad \left. \cdot \frac{c_i^l}{a^{l+2}} \cdot (2l+1) \cdot P_l(\cos \beta_i) \right] \cdot P_l(\cos \theta) \end{aligned} \quad (14)$$

Similarly, the current density at the external surface of the membrane obeys

$$\begin{aligned} i_o(\theta) &= -\gamma_o \cdot \nabla V|_{r \rightarrow a^-} \\ &= \gamma_o \cdot \sum_{l=0}^{\infty} \left[B_l \cdot (l+1) \cdot a^{-(l+2)} - \frac{q_o}{4\pi\gamma_o} \right. \\ &\quad \left. \cdot \frac{a^{l-1}}{c_o} \cdot (2l+1) \cdot P_l(\cos \beta_o) \right] \cdot P_l(\cos \theta) \end{aligned} \quad (15)$$

The current density inside $i_i(\theta)$ and outside $i_o(\theta)$ have to be equal, i.e., $i_i(\theta) = i_o(\theta) = i(\theta)$. Additionally, we will assume that the external electrode carries the same current as the intracellular electrode, only scaled by the factor v . Thus we

define

$$\begin{aligned} q &:= q_i \\ q_o &:= v \cdot q \\ \beta &:= \beta_o \end{aligned} \quad (16)$$

The equality of $i_i(\theta)$ and $i_o(\theta)$ corresponding to Eqs. 14 and 15 allows us to express the coefficients B_l in terms of A_l , q , and v , yielding

$$\begin{aligned} B_l &= \frac{a^{l+2}}{l+1} \cdot \left\{ -\frac{\gamma_i}{\gamma_o} \cdot \left[A_l \cdot l \cdot a^{l-1} - \frac{q}{4\pi\gamma_i} \cdot \frac{c_i^l}{a^{l+2}} \cdot (2l+1) \right] \right. \\ &\quad \left. + \frac{v \cdot q}{4\pi\gamma_o} \cdot \frac{a^{l-1}}{c_o} \cdot (2l+1) \cdot P_l(\cos \beta) \right\} \\ &= -\frac{\gamma_i}{\gamma_o} \cdot A_l \cdot \frac{l}{l+1} \cdot a^{2l+1} + \frac{\gamma_i}{\gamma_o} \cdot c_i^l \cdot \frac{q}{4\pi\gamma_i} \cdot \frac{2l+1}{l+1} \\ &\quad + \frac{v \cdot q}{4\pi\gamma_o} \cdot \frac{a^{2l+1}}{c_o} \cdot \frac{2l+1}{l+1} P_l(\cos \beta) \end{aligned} \quad (17)$$

To obtain a full solution for the potential behavior we additionally require boundary conditions relating the potentials at the membrane surfaces.

Boundary conditions for fast charging of the membrane

In the case of fast charging of the membrane the membrane conductance is negligible in comparison with the admittance due to the capacitance. Thus we may assume the membrane to have infinitely high resistance, and the current charges the membrane as an ideal capacitor,

$$\frac{d\Phi(\theta)}{dt} = \frac{d(V_i(\theta) - V_o(\theta))}{dt} = \frac{1}{c} \cdot i(\theta) \quad (18)$$

with c denoting the capacitance per unit area of the membrane and $\Phi(\theta)$ denoting the transmembrane potential. This is equivalent to the small ϵ and short-time solutions considered by Peskoff and Eisenberg (1975) and Peskoff and Ramirez (1975). Inserting the definitions of $V_i(\theta)$ and $V_o(\theta)$ from Eqs. 7 and 8 and the equation for the current density (Eq. 14) into Eq. 18 yields the following differential equation

$$\begin{aligned} &\sum_{l=0}^{\infty} \frac{dA_l}{dt} \cdot a^l \cdot P_l(\cos \theta) \\ &+ \frac{\gamma_i}{\gamma_o} \cdot \sum_{l=0}^{\infty} \frac{dA_l}{dt} \cdot \frac{l}{l+1} \cdot a^l \cdot P_l(\cos \theta) \\ &- \frac{\gamma_i}{\gamma_o} \sum_{l=0}^{\infty} \frac{dq}{dt} \cdot \frac{c_i^l}{4\pi\gamma_i} \cdot \frac{2l+1}{l+1} \cdot a^{-(l+1)} \cdot P_l(\cos \theta) \\ &- \frac{v}{4\pi\gamma_o} \cdot \sum_{l=0}^{\infty} \frac{dq}{dt} \cdot \frac{a^l}{c_o} \cdot \frac{2l+1}{l+1} \cdot P_l(\cos \beta) \cdot P_l(\cos \theta) \end{aligned} \quad (19)$$

$$= -\frac{\gamma_i}{c} \cdot \sum_{l=0}^{\infty} \left[A_l \cdot l \cdot a^{l-1} - \frac{q}{4\pi\gamma_i} \cdot \frac{c_i^l}{a^{l+2}} \cdot (2l+1) \right] \cdot P_l(\cos \theta)$$

The above equation (19) has to be fulfilled at each angle θ and for all indices l . Thus one obtains an infinite system of ordinary differential equations for the coefficients A_l as

$$\frac{dA_l}{dt} = E_l \cdot \left(F_l \cdot A_l + G_l \cdot \frac{dq}{dt} + H_l \cdot q \right) \quad (20)$$

with the abbreviations

$$E_l := \left[a^l \cdot \left(1 + \frac{\gamma_i}{\gamma_o} \cdot \frac{l}{l+1} \right) \right]^{-1}$$

$$F_l := -\frac{\gamma_i \cdot l \cdot a^{l-1}}{c}$$

$$G_l := \frac{c_i^l \cdot (2l+1)}{4\pi\gamma_o \cdot a^{l+1} \cdot (l+1)} + \frac{v \cdot a^l \cdot (2l+1)}{4\pi\gamma_o \cdot c_o \cdot (l+1)} \cdot P_l(\cos \beta)$$

$$H_l := \frac{c_i^l \cdot (2l+1)}{4\pi \cdot c \cdot a^{l+2}}$$

The parameters that are adjustable are the position c_o of the compensation electrode and the scaling factor v for the current it injects. To find “optimal” values for these two parameters we must first define an optimality criterion.

Optimality criterion

The fastest and most appropriate form of current injection would be a delta pulse of current. For an ideal, homogeneous capacitor this would yield a step change in the potential. If the voltage clamp system is optimally adjusted for the response to a delta function of current, it is well-adjusted for any fast current injections. Therefore we calculate the solution of Eq. 20 for

$$q = Q \cdot \delta(t) \quad (21)$$

given an initial membrane potential that is zero. The solution turns out to be

$$A_l = Q \cdot e^{E_l F_l t} \cdot (E_l F_l G_l + E_l H_l) + \delta(t) \cdot E_l G_l \cdot Q$$

with the l -dependent factors as defined above. The interesting part of the impulse response is only for $t > 0$, i.e.,

$$A_l = Q \cdot e^{E_l F_l t} \cdot (E_l F_l G_l + E_l H_l) \quad (22)$$

with the decay constants

$$E_l F_l = -\frac{\gamma_i \cdot l}{c \cdot a \cdot \left(1 + \frac{\gamma_i}{\gamma_o} \cdot \frac{l}{l+1} \right)} \quad (23)$$

(Hellerstein, 1968; Peskoff and Ramirez, 1975). In order to optimize the voltage clamp setup one may decide to minimize the deviation of the impulse response from the ideal,

homogeneous one corresponding to A_0 (the time constant $E_1 F_1 = 0$ for $l = 0$). Thus we minimize the integral over time and the cell surface of the squared deviation of the membrane potential from the homogeneous (steplike) potential change

$$\int_t \int_A (\Phi - \bar{\Phi})^2 dA dt \quad (24)$$

Here $\bar{\Phi}$ denotes the homogeneous (uniform) part of the transmembrane potential, i.e.,

$$\bar{\Phi} = \frac{Q}{4\pi \cdot c \cdot a^2} \quad (25)$$

Using the representation with Legendre polynomials and the fact that the surface element is

$$dA = 2\pi a^2 \cdot \sin \theta d\theta$$

we obtain

$$\int_t \int_A (\Phi - \bar{\Phi})^2 dA dt = 2\pi a^2 \cdot \int_0^\infty \int_0^\pi \sin \theta \cdot \left[\sum_{l=1}^\infty (A_l \cdot a^l - B_l \cdot a^{-(l+1)}) \cdot P_l(\cos \theta) \right]^2 d\theta dt \quad (26)$$

It can be shown that the Legendre polynomials have the nice property that

$$\int_0^\pi \sin \theta \cdot P_l(\cos \theta) \cdot P_k(\cos \theta) d\theta = 0 \quad \text{for } l \neq k$$

Thus we may rewrite Eq. 26 in

$$\begin{aligned} & 2\pi a^2 \cdot \int_0^\infty \int_0^\pi \sin \theta \cdot \sum_{l=1}^\infty (A_l \cdot a^l - B_l \cdot a^{-(l+1)})^2 \cdot P_l^2(\cos \theta) d\theta dt \\ &= 2\pi a^2 \cdot \int_0^\infty \left[\sum_{l=1}^\infty (A_l \cdot a^l - B_l \cdot a^{-(l+1)})^2 \cdot \int_0^\pi \sin \theta \cdot P_l^2(\cos \theta) d\theta \right] dt \quad (27) \\ &= 2\pi a^2 \cdot \int_0^\infty \sum_{l=1}^\infty (A_l \cdot a^l - B_l \cdot a^{-(l+1)})^2 \cdot \frac{2}{2l+1} dt \end{aligned}$$

The last step uses

$$\int_0^\pi \sin \theta \cdot P_l^2(\cos \theta) d\theta = \frac{2}{2l+1}$$

The injected current $q = 0$ for all times $t > 0$. Thus it follows from Eq. 17 that

$$(A_l \cdot a^l - B_l \cdot a^{-(l+1)})^2 = A_l^2 \cdot a^{2l} \cdot \left[1 + \frac{\gamma_i}{\gamma_o} \cdot \frac{l}{l+1} \right]^2 \quad (28)$$

leading to

$$\begin{aligned} & \int_t \int_A (\Phi - \bar{\Phi})^2 dA dt \\ &= 2\pi a^2 \cdot \int_0^\infty \sum_{l=1}^\infty (A_l \cdot a^l - B_l \cdot a^{-(l+1)})^2 \cdot \frac{l}{2l+1} dt \quad (29) \\ &= -2\pi a^2 \cdot \sum_{l=1}^\infty (E_l F_l G_l + H_l)^2 \\ & \quad \cdot \left(1 + \frac{\gamma_i}{\gamma_o} \cdot \frac{l}{(l+1)} \right)^2 \cdot \frac{E_l}{F_l} \cdot \frac{a^{2l}}{2l+1} \end{aligned}$$

An expression for the cost function CF to be minimized is therefore

$$CF := - \sum_{l=1}^\infty (E_l F_l G_l + H_l)^2 \cdot \left(1 + \frac{\gamma_i}{\gamma_o} \cdot \frac{l}{(l+1)} \right)^2 \cdot \frac{E_l}{F_l} \cdot \frac{a^{2l}}{2l+1} \quad (30)$$

As the above series converges rather quickly, it is sufficient for the optimization to sum ~ 40 terms, rendering standard numerical optimization algorithms applicable. Closer analysis of the cost function reveals that it is scaled by the specific capacitance of the membrane, but changes in c have no influence on the optimum values of v and c_a .

Stationary solution of the field problem

In the case that the conductivity of the membrane is high, the constant holding current required to clamp the voltage will cause non-negligible nonuniformities in the transmembrane potential. To calculate the potential in the stationary case, one has to solve

$$i(\theta) - \gamma_m \cdot \Phi(\theta) = i(\theta) - \gamma_m \cdot (V_i(\theta) - V_o(\theta)) = 0 \quad (31)$$

with $\Phi(\theta)$ denoting the transmembrane potential (i.e., $\Phi(\theta) = V_i(\theta) - V_o(\theta)$) and γ_m denoting the specific conductivity of the membrane. Using the variables introduced above, this equation can be rewritten as

$$\begin{aligned} & \gamma_i \cdot \sum_{l=0}^\infty \left[A_l \cdot l \cdot a^{l-1} - \frac{q}{4\pi\gamma_i} \cdot \frac{c_i^l}{a^{l+2}} \cdot (2l+1) \right] \cdot P_l(\cos \theta) \\ & - \gamma_m \cdot \sum_{l=0}^\infty [A_l \cdot a^l - B_l \cdot a^{-(l+1)}] \cdot P_l(\cos \theta) = 0 \quad (32) \end{aligned}$$

leading to

$$A_1 = \frac{q}{4\pi\gamma_i} \cdot \frac{\mathcal{A}}{a^l \cdot \left[\frac{\gamma_i \cdot l}{a} + \gamma_m \cdot \left(1 + \frac{\gamma_i}{\gamma_o} \cdot \frac{l}{l+1} \right) \right]} \quad (33)$$

where

$$\mathcal{A} = \frac{c_i^l}{a^{l+1}} \cdot \left[\frac{\gamma_i \cdot (2l+1)}{a} + \gamma_m \cdot \frac{\gamma_i}{\gamma_o} \cdot \frac{2l+1}{l+1} \right] + \frac{v \cdot \gamma_i}{\gamma_o} \cdot \gamma_m \cdot \frac{a^l}{c_o} \cdot \frac{2l+1}{l+1} \cdot P_1(\cos \beta)$$

Using these values for A_1 one may calculate B_1 from Eq. 17 and obtain the stationary membrane potential as

$$\Phi(\theta) = \sum_{l=0}^{\infty} [A_l a^l - B_l a^{-(l+1)}] P_l(\cos \theta) \quad (34)$$

As will be shown below, a setup optimized using the above cost function CF (Eq. 30) yields excellent results even for a stationary holding current in the case of high expression level. Thus an additional optimality criterion that would have to include the membrane conductivity is not necessary.

MATERIALS AND METHODS

Numerical computations

Numerical calculations were carried out using MATLAB 4.2c1 (Math Works, Natick, MA) on a 486 computer, or MATLAB 5.1 on a Power Macintosh computer. Summation of spherical harmonics was carried out to 40 terms except in the case of the potential plots in Figs. 7 and 8, where 100 terms were summed with a cosine taper applied to the last 50 terms.

Oocyte preparation

Oocytes were removed from adult female *Xenopus laevis* frogs anesthetized with 0.2% tricaine (Sigma Chemical Co., St. Louis, MO), and defolliculated with 2 mg/ml collagenase (Type 1A; Sigma Chemical Co.) in OR-2 solution, which contains (in mM): 82.5 NaCl, 2 KCl, 1 MgCl₂, and 5 HEPES; pH 7.5 adjusted with NaOH. Oocytes were stored at room temperature in ND96 containing (in mM) 96 NaCl, 2 KCl, 1.8 CaCl₂, 1 MgCl₂, and 5 HEPES; pH 7.5 was adjusted with NaOH. For storage of oocytes the solution was supplemented with 100 U/ml penicillin and 100 μg/ml streptomycin. All measurements were performed on healthy stage V–VI oocytes in ND96.

Determination of oocyte parameters

The specific conductivity of the oocytes' cytosol was measured by methods similar to those of Cole (1928). A chamber as depicted in Fig. 2 A was assembled to measure the frequency-dependent impedance of a cell suspension. Chlorided silver plates were mounted at opposite walls of a plastic cuvette with base dimensions of 10 × 10 mm. These electrodes were covered with filter paper to prevent physical contact with the oocytes. The voltage drop across the cell suspension was measured with two chlorided silver wires mounted directly at the surface of the covered plate electrodes. Oocytes suspended in fresh ND96 solution were introduced into the chamber to 12 mm height, and maintained in suspension by agitation. A sinusoidal voltage $V_0 = 2$ V peak-to-peak was applied to the plate elec-

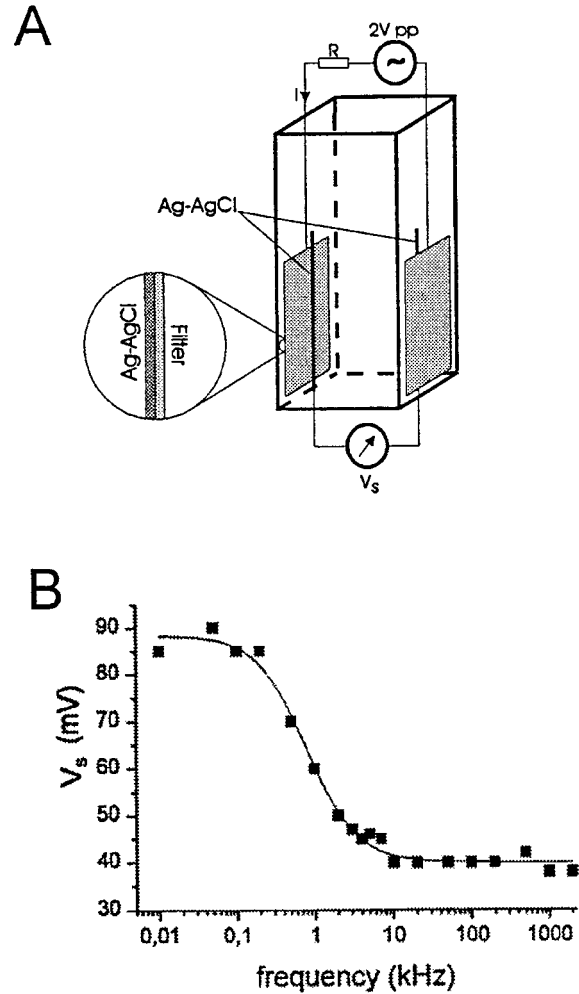


FIGURE 2 Measurement of the cytosolic conductivity. The chamber (A) was filled to a height of 12 mm with ND96 solution or a suspension of cells in ND96. A sinusoidal voltage (2 V peak-to-peak) was applied through a series resistance $R = 10$ k Ω and its frequency was varied from 100 Hz to 2 MHz as the voltage drop V_s over the chamber was measured. For the oocyte suspension this yielded the frequency-voltage relation in (B). The smooth curve is a fit according to Eq. 35.

trodes via a series resistor R of 10 k Ω and the frequency was varied from 100 Hz to 2 MHz. The frequency dependence of the measured voltage V_s follows to be

$$V_s(f) = \frac{|Z|}{|Z + R|} V_0 \quad (35)$$

with Z denoting the total impedance of the cell suspension.

Microelectrode measurements

We modified a commercially available two-electrode voltage clamp amplifier (OC-725A; Warner Instruments, Hamden, CT). The variable-gain amplifier output was connected to a home-made head stage consisting of two voltage-to-current converters. One of these voltage-to-current converters was connected to the current-injecting electrode and the second to the compensation electrode. Voltage-sensing and current-injecting microelectrodes were pulled from borosilicate glass (Kimax, Corning) and filled with 3 M KCl resulting in a final resistance of ~ 1 M Ω . The pipettes for the

compensation electrode were pulled as the other two electrodes, but then the tip was broken and fire-polished before filling with 3 M KCl, yielding a resistance of ~ 50 k Ω . To avoid problems in long-lasting experiments caused by KCl leakage out of the compensation electrode either continuous extracellular perfusion or an agarose cushion (Schreibmayer et al., 1994) in the compensation pipette should be used. However, for the short-duration experiments reported here we did not take these precautions.

All electrodes were coated with Polystyrene Q-Dope (GC Electronics) to reduce capacitive coupling. Furthermore, the distance of the retracted Q-Dope from the tip was measured in a calibrated microscope allowing for an optical determination of penetration depth and the distance of the compensation electrode from the cell membrane.

A "delta function" of current was programmed as a 20- μ s pulse, delivered from the Pulse program (HEKA Elektronik, Lambrecht, Germany) through an ITC-16 interface (InstruTech) directly to the current-to-voltage converters. After recording the averaged response from the voltage-sensing microelectrode, that microelectrode was withdrawn to just outside the membrane surface and a second set of responses was averaged to estimate the artifact due to capacitive coupling and series resistance. The difference between the two average responses was taken to be the membrane potential response to the injected current.

RESULTS

Passive properties of oocytes

To apply the theory derived above we first determined the values of the cytosolic conductivity γ_i , the bath conductivity γ_o , and the specific membrane capacity c of representative oocytes. The cytosolic conductivity was determined using the chamber depicted in Fig. 2 A. Initially the chamber was filled with pure ND96 and no frequency dependence was observed of the voltage drop over the bath (V_S) which was 19 mV. From this the resistance of the bath was computed according to Eq. 35 to be 96 Ω , yielding the specific conductivity $\gamma_o = 1.2$ S/m. The experiment was then repeated with the suspension of oocytes in ND96. The measured relationship between frequency and V_S is shown in Fig. 2 B. At low frequencies the oocytes are essentially insulating spheres, due to the low membrane conductance. Given a volume fraction p of oocytes, the complex specific impedance of the cell suspension is given by

$$z = \gamma_o \frac{(1-p)\gamma_o + (2+p)[\gamma_i^{-1} + (j2\pi fca)^{-1}]}{(1+2p)\gamma_o + 2(1-p)[\gamma_i^{-1} + (j2\pi fca)^{-1}]} \quad (36)$$

(Cole, 1928). With the oocyte radius ~ 0.55 mm, nonlinear least-square fitting of this equation to the data in Fig. 2 B yielded the volume fraction $p = 0.79 \pm 0.04$, cytosolic conductivity $\gamma_i = 0.24 \pm 0.03$ S/m, and membrane capacitance $c = 45.6 \pm 5$ mF/m². This last value is in excellent agreement with the value obtained from single cell charge-voltage curves ($c = 47.2$ mF/m²). The cytosolic conductivity is therefore a factor of 5 smaller than that of the bath solution. The membrane capacitance is 6.5 times larger than expected for a lipid bilayer (7 mF/m²), reflecting the highly folded oocyte membrane that is seen to contain many microvilli (Soreq and Seidman, 1992).

Optimal setup

The large potential errors shown below can be reduced by reducing the membrane current; for example, a reduction by a factor of 10 results in membrane potential errors that are smaller by slightly more than a factor of 10. Alternatively, one expects that by appropriate electrode configurations the spatial variations in electric field could be reduced. A solution is to place the current-passing electrode close to the center of the oocyte. Indeed, better performance is observed in the two-microelectrode voltage clamp when the tip of the current-passing microelectrode is driven to the center of the oocyte (S. H. Heinemann, personal communication), resulting in spherically symmetric current flow. As the electrode is driven closer to the center, the inhomogeneity becomes much smaller. However, because driving a glass microelectrode deep into the cell causes a large leak conductance, we sought other modifications to the basic voltage clamp setup to improve the electric field distribution. One thought was to place the external bath electrode close to the oocyte, but as far as possible from the current-passing electrode. Although this causes an increase in field strength at the opposite pole of the oocyte and is therefore a change in the right direction, it does not solve the main problem of the very strong concentration of field close to the current-passing electrode.

The best solution we found was to introduce an additional "compensating" electrode, which is placed outside the oocyte in the vicinity of the current-passing microelectrode. We derived the theory for a general ring-shaped electrode, but obtain the optimum performance when the electrode is a point source of current, i.e., $\beta = 0$. However, a small ring could be a desirable configuration for technical simplicity (for example, a plated pipette or a concentric electrode) and yields only slightly worse results (data not shown).

The correct compensation depends strongly on the position c_o and the amplification factor v of current passed through this electrode. Fig. 3 shows the dependence of the logarithm of the optimization function CF according to Eq. 30 on these variables, assuming a penetration depth of 100 μ m, a diameter of 1.3 mm, and using the parameters of the

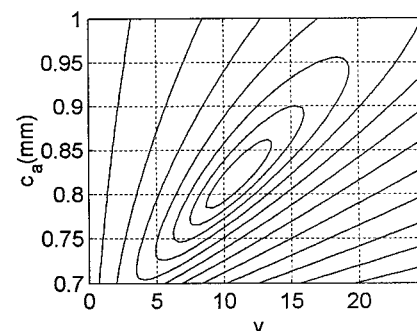


FIGURE 3 The dependence of the logarithm of the cost function CF on the position (c_o) of the compensation electrode and the compensation factor v . A minimum occurs at $c_o \approx 0.825$ mm and $v \approx 12$. The oocyte radius was assumed to be $a = 0.65$ mm and the microelectrode penetration depth was 100 μ m.

TABLE 1 The optimal distance of the compensation electrode from the membrane $\delta_o = c_o - a$ (in μm) and the optimal gain v are shown in dependence on the radius of the oocyte a and on the penetration depth $\delta_i = a - c_i$

a (mm)	δ_o (μm)/ v				
	$\delta_i = 50 \mu\text{m}$	100 μm	150 μm	200 μm	250 μm
0.25	90.3/14.5	243.9/24.7	532.0/42.1	1361.2/89.7	—/0
0.30	85.5/13.1	220.4/20.9	433.2/32.0	840.1/51.9	2026.8/108.3
0.35	81.9/12.1	205.6/18.5	382.9/26.6	665.6/38.8	941.2/61.5
0.40	79.1/11.3	195.0/16.8	352.0/23.3	577.6/32.0	941.2/45.4
0.45	76.8/10.8	187.0/15.5	330.6/20.9	524.1/27.7	804.6/37.1
0.50	75.0/10.3	180.7/14.5	314.9/19.2	487.8/24.8	722.0/32.0
0.55	73.4/9.9	175.4/13.7	302.6/17.9	461.2/22.6	666.3/28.5
0.60	72.2/9.6	170.9/13.1	292.6/16.8	440.9/20.9	626.0/25.9
0.65	71.2/9.4	167.1/12.4	284.3/15.9	424.6/19.6	595.3/23.8
0.70	70.3/9.2	163.7/12.1	277.2/15.2	411.1/18.5	571.0/22.3

The ratio of the bath conductivity and the cytosolic conductivity is assumed to be 5.

oocyte as described above. An optimum occurs at $c_o \approx 0.825$ mm and $v \approx 12$. It can be seen that there is a relatively long valley in the function $\log(CF)$, implying that the choice of one parameter, say c_o , is not critical provided that the other parameter is adjusted correspondingly. This is useful because v can be easily adjusted by a potentiometer, while changing c_o requires mechanical modification of the system. The optimum values of c_o and v depend on the particular penetration depth, as shown in Table 1. Although the optimization is carried out for fast charging of the membrane, the performance of the setup is very good for steady-state currents as well, as will be shown below.

Time-dependent errors in membrane potential

Peskoff and Ramirez (1975) have shown that a step-function of injected current produces a short-term relaxation of membrane potential in a spherical cell that is much faster than the membrane time constant. We consider the case of current injection that is a delta function of time, because when a voltage clamp system is commanded to produce a step change in membrane potential, a brief pulse of current is injected through the current-passing microelectrode. As shown in Fig. 4, a delta function of current injected into a cell the size of an oocyte results in large transient errors in membrane potential that decay with time. For a current pulse that produces a 100-mV step, an error of nearly 700 mV is observed in the vicinity of the current-injecting electrode 50 μs after the current pulse, and errors of 20 mV persist after 400 μs .

The potential distribution can be expressed as a series in which the spatial component of each term is a spherical harmonic and the temporal dependence is a decaying exponential of time (Eq. 22). For the l th term the time constant is seen from Eq. 23 to be approximately

$$\tau_l \approx \frac{ca}{\gamma_l l}$$

where c is the specific membrane capacitance and a the cell radius. The term with $l = 0$ corresponds to the mean

(spherically symmetric) change in membrane potential, which does not decay with time. For our standard oocyte parameters the $l = 1$ term (corresponding to the spatial component of the form $\cos(\theta)$) has a time constant $\tau_1 = 150$

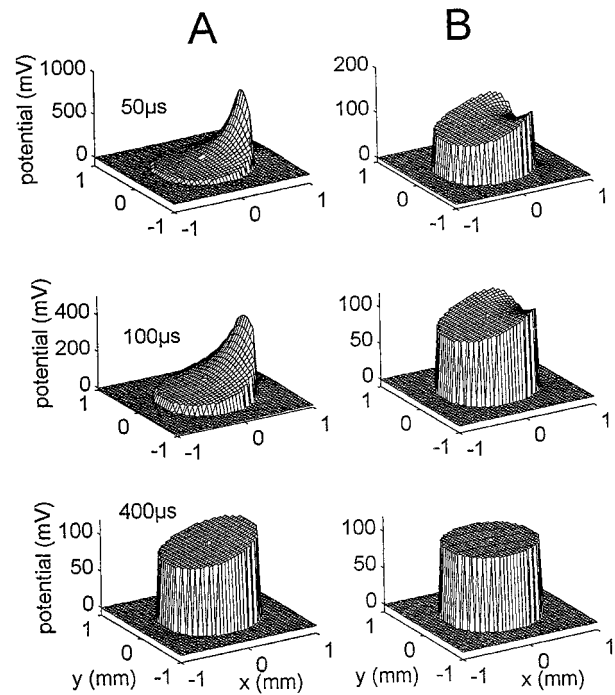


FIGURE 4 Redistribution of membrane potential after an injected current pulse using a single current-passing microelectrode (A) and with the addition of the compensation electrode (B). The potential distribution inside and outside an oocyte after a pulse of injected current was computed according to Eqs. 17, 22, and 34. The oocyte is assumed to be a sphere of radius 0.65 mm centered on the origin. The current source is located at $r = 0.55$ mm and $\theta = 0$, i.e., 100 μm from the membrane inside the oocyte. The potential distribution is shown (top to bottom) 50, 100, and 400 μs after a short pulse of current that charges the mean membrane potential to 100 mV. In the uncompensated case the maximum deviation from isopotentiality 100 μs after the pulse is ~ 300 mV, whereas the compensation reduces this maximum deviation to ~ 17 mV. Even after 400 μs the maximum potential deviation is still ~ 10 mV if the conventional setup is used, whereas the compensation reduces this error to ~ 1 mV.

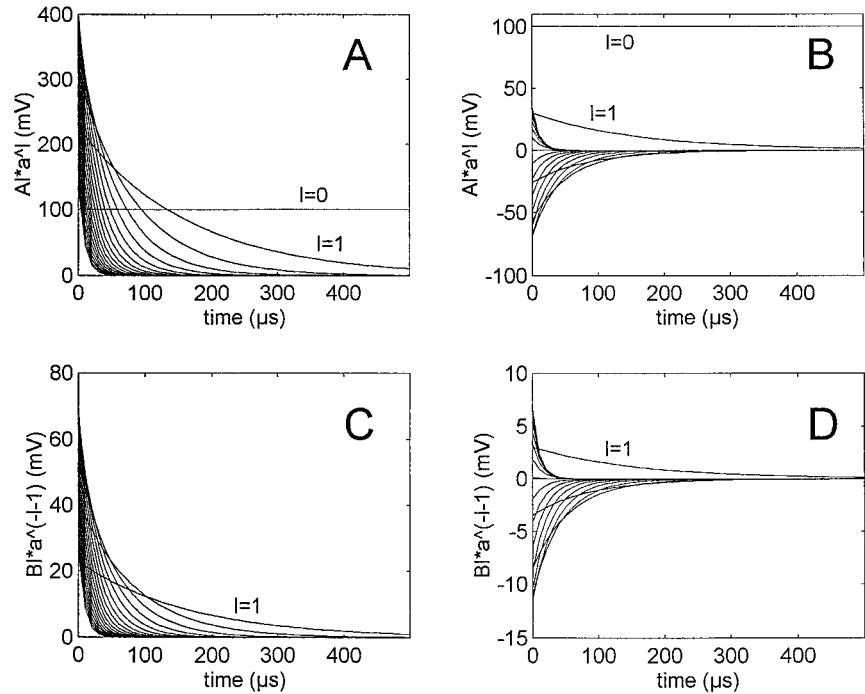


FIGURE 5 The time course of decay of the coefficients $A_l \cdot a^l$ and $B_l \cdot a^{l-1}$ that determine the membrane potential (Eq. 34) after a delta pulse of current that charges the mean membrane potential to 100 mV. The time courses of the coefficients are shown without compensation (A and C) and with compensation (B and D).

μs . This time constant places a fundamental limit on the speed of membrane potential settling, a limit which can be avoided only if the amplitude of this term is small. Fig. 5 A shows the amplitudes of the first 20 terms as a function of time in the case of the standard voltage clamp system. The $l = 1$ term has a large amplitude, initially twice that of the desired membrane potential change, such that the settling of the membrane potential will take several hundreds of microseconds.

With optimum adjustment of the compensating electrode the amplitudes of all terms are decreased by more than an order of magnitude, as can be seen in Fig. 5 B; an exception is the desired $l = 0$ term, which is unchanged. This means that considerably faster settling of the membrane potential is obtained with the compensating electrode.

As an experimental test of the theory we measured the voltage response of an uninjected oocyte to a short (20- μs) pulse of current applied in the presence of a compensating electrode (Fig. 6). The membrane potential was measured at the angles $\theta = 180^\circ$ and 30° as the compensation factor ν was varied from zero to 20. The artifacts due to capacitive coupling between the electrodes and series resistance in the bath were mostly removed by subtracting the voltage response recorded after withdrawal of the voltage-sensing electrode from the oocyte.

The current-injecting electrode was inserted into the oocyte at a small angle of $\sim 15^\circ$ to the membrane normal, while the compensation electrode was positioned radially outside the cell. This arrangement minimized the possible "shadow effect" on the electric field due to the current-injecting electrode pipette. We ignored this effect in our calculations but expect it to be small because of the small solid angle subtended by the microelectrodes.

With no compensation ($\nu = 0$) the time course of membrane potential shows a gradual rise when recorded at $\theta = 180^\circ$, but an overshoot is seen in the recording at $\theta = 30^\circ$. The effect of increasing ν is to counteract this behavior, with the desired step function best approximated by the curve with $\nu = 10$, similar to the expected optimum value. The recordings of membrane potential are well-matched by the theoretical time courses, which were computed with no free parameters.

Steady-state voltage clamp

When oocytes are expressing high densities of channel proteins it is not uncommon to record membrane currents of 100 μA or more. The steady-state potential, computed using the coefficients given in Eq. 33, is shown in Fig. 7 for the case of 100 μA of injected current in a cell with the large membrane conductance of 1 mS. In the uncompensated case (Fig. 7 A) the large potential near the site of current injection results in a local membrane potential 600 mV greater than the average value. The very large local potential explains a common experimental observation, that passing large currents into oocytes results in membrane damage. Use of a compensation electrode (Fig. 7 B) produces an extracellular potential gradient that mirrors the intracellular gradient, largely canceling the inhomogeneity of membrane potential. The effect on local membrane potential can be seen more clearly in Fig. 8 A, where membrane potential is plotted as a function of the angle θ . At an injected current of 100 μA the local membrane potential near the current-injection site ($\theta = 0$) is 750 mV; at the opposite pole of the cell it is 50 mV; the mean potential (obtained as the $l = 0$ term in the

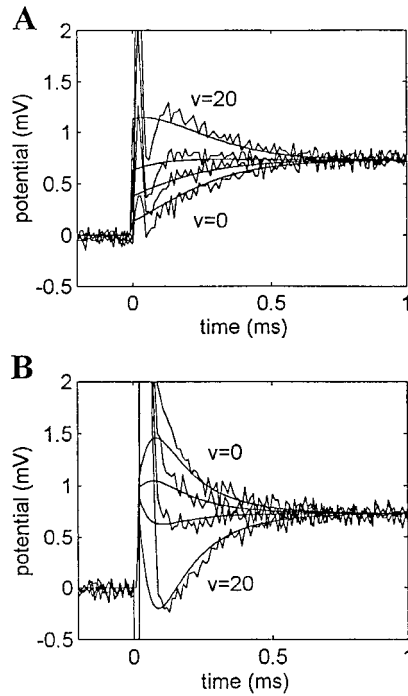


FIGURE 6 Theoretical and experimentally observed time course of the membrane potential of an oocyte. A 20- μ s pulse of current was injected through a microelectrode driven 0.1 mm into an oocyte of diameter 1.36 mm. The membrane potential measured at $\theta = 180^\circ$ (A) and $\theta = 30^\circ$ (B) was recorded. The compensation electrode was positioned at $c_o \approx 0.8$ mm and the gain v was adjusted to 0, 5, 10, and 20. The smooth curves are the predicted membrane potential from Eqs. 17, 22, and 34, corresponding to the experimental situation.

expansion of the membrane potential) is 100 mV in this case. The effect of the compensation electrode (Fig. 8 B) is to reduce the maximum deviation in membrane potential by a factor of 20.

With the standard geometry assumed here and under the conditions of optimal compensation, the compensation electrode carries a current $v = 12$ times larger than the current actually injected into the cell by the current-passing microelectrode. Why is such a large current necessary? The large value of v can be understood in part from the large ratio, a factor of 5, between the cytoplasmic and external conductivities. A current at least five times as large is required to produce the same field strength in the external solution as exists in the cytoplasm due to the current-passing microelectrode.

The extra current through the compensating electrode increases the potential drop in the bath solution, in effect increasing the series resistance between the extracellular membrane surface and the bath electrode. Assuming a large bath electrode at $r = \infty$, evaluation of the $l = 0$ term of the extracellular potential yields the effective series resistance

$$R_s = \frac{1}{4\pi\gamma_o} \left(\frac{1}{a} + \frac{v}{c_o} \right) \quad (37)$$

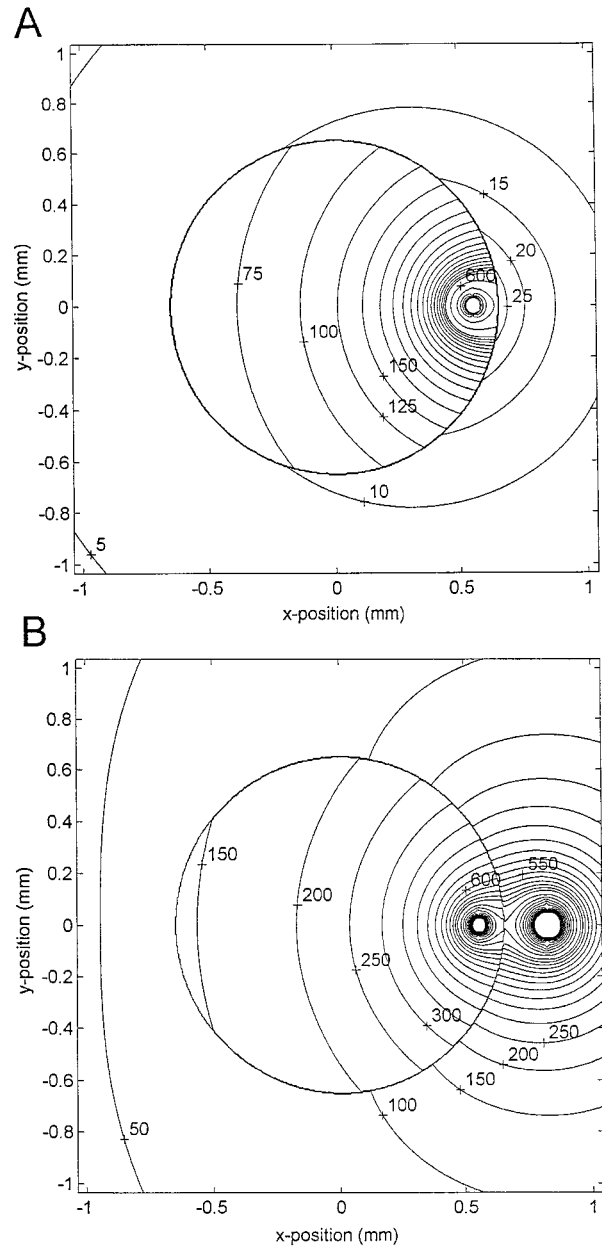


FIGURE 7 Steady-state potential distribution due to current injection. Isopotential contours (labeled in units of mV) are shown inside and outside a spherical cell of radius 0.65 mm when a current of 100 μ A is injected from a point source located at a depth $\delta = 0.1$ mm beneath the membrane. The total membrane conductance is taken to be 1 mS; the cytoplasmic conductivity $\gamma_i = 0.25$ S/m and bath conductivity $\gamma_o = 1.25$ S/m. (A) Potential in the standard configuration; (B) potential distribution in the presence of the compensation electrode, with an extracellular compensation electrode located at radius $c_o = 0.825$ mm and driven with a current $v = 12$ times larger than the 100 μ A current injected intracellularly. The contour intervals in (A) are 5 mV (up to 25 mV), 25 mV (up to 500 mV), and 100 mV (up to 1500 mV). In (B) the contour intervals are 50 mV (up to 800 mV) and 100 mV (up to 2000 mV).

Given the oocyte parameters used here this resistance is 120 Ω in the absence of compensation; with compensation it is 1220 Ω . Thus, electronic compensation for R_s will be required in a practical voltage clamp system employing the compensation electrode.

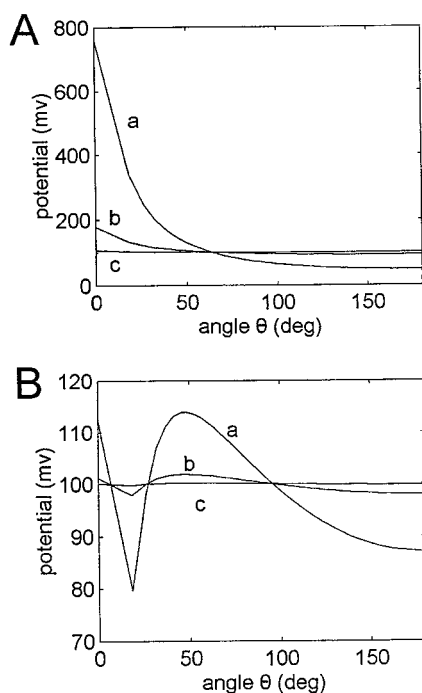


FIGURE 8 Transmembrane potential as a function of the angle θ without (A) and with (B) compensation. The curves are calculated for membrane conductivities of 1 mS (a), 0.1 mS (b), and 0.01 mS (c) and a current that displaces the mean membrane potential to +100 mV.

DISCUSSION

It has been known for many years that the injection of current from an eccentrically placed microelectrode can result in inhomogeneous membrane potentials in spherical cells (Rall, 1953; Eisenberg and Engel, 1970). In most cell types this issue is unimportant because the magnitude of the effect is small and the time constants of relaxations are rapid. In the *Xenopus* oocyte system, however, the effects provide severe limitations on voltage clamp performance. The combination of large-diameter, low-cytoplasmic conductivity and a high degree of membrane infolding in these cells yields large membrane potential errors from eccentrically injected current. These errors are time-dependent, relaxing with a maximum time constant of $\sim 150 \mu\text{s}$; they also become very large in the steady state when large membrane currents are flowing. In view of these errors, it is seen that in the conventional two-microelectrode voltage clamp the oocyte membrane cannot be considered to be isopotential on time scales of 300 μs or less, or when the total current is larger than $\sim 20 \mu\text{A}$.

These membrane potential errors can be reduced by placing the current-passing electrode near the center of the cell. We expect that an important reason why the cut-open oocyte technique (Tagliatalata et al., 1992) provides a faster and much higher fidelity voltage control than the two-microelectrode voltage clamp is its improved geometry of current injection. The injected current comes either from an electrode placed near the center of the oocyte or through a

large area of permeabilized membrane. The result is that the radius c_i of current injection is small, resulting in small values of all coefficients with $l > 0$ for both the steady-state and the transient deviations in membrane potential.

In seeking to improve the two-microelectrode voltage clamp, we considered various electrode configurations and found that an extracellularly placed "point source" of injected current is the best configuration for an electrode that compensates for errors from the eccentrically injected current. This extracellular electrode makes for more uniform current flow and can reduce the size of transient errors by an order of magnitude. The optimal placement of this electrode depends on the depth of penetration of the intracellular current-injecting electrode; however, this placement is relatively noncritical when the magnitude of injected current can be adjusted for optimum voltage uniformity. In practice this adjustment can be made to minimize the slow relaxations in current clamp responses or in the capacitive current in voltage clamp recordings.

We thank V. Pantani for construction of the modified voltage clamp amplifier.

This work was supported by National Institutes of Health Grant NS21501, the Austrian Research Funds (Project S6609), and the Deutsche Forschungsgemeinschaft (SFB 176).

REFERENCES

- Abraham, M., and R. Becker. 1950. *Classical Electricity and Magnetism*. Blackie & Son, Ltd. London, England. 114.
- Abramowitz, M., and I. A. Stegun. 1972. *Handbook of Mathematical Functions*. Dover Publications, Inc., New York.
- Cole, K. S. 1928. Electric impedance of suspensions of *Arabicia* eggs. *J. Gen. Physiol.* 12:37-54.
- Cole, K. S. 1949. Dynamic electrical characteristics of the squid axon membrane. *Arch. Sci. Physiol.* 3:253-258.
- Eisenberg, R. S., and E. Engel. 1970. The spatial variation of membrane potential near a small source of current in a spherical cell. *J. Gen. Physiol.* 55:736-757.
- Eisenberg, R. S., and E. A. Johnson. 1970. Three-dimensional electric field problems in physiology. *Prog. Biophys. Mol. Biol.* 20:1-65.
- Gundersen, C. B., R. Miledi, and I. Parker. 1983. Serotonin receptors induced by exogenous messenger RNA in *Xenopus* oocytes. *Proc. R. Soc. Lond. B.* 219:103-109.
- Gurdon, J. B., C. D. Lane, H. R. Woodland, and G. Marbaix. 1971. Use of frog eggs and oocytes for the study of messenger RNA and its translation in living cells. *Nature.* 233:177-182.
- Hellerstein, D. 1968. Passive membrane potentials. *Biophys. J.* 8:358-378.
- Hodgkin, A. L., A. F. Huxley, and B. Katz. 1949. Ionic current underlying activity in the giant axon of the squid. *Arch. Sci. Physiol.* 3:129-150.
- Jackson, J. D. 1962. *Classical Electrodynamics*. Wiley, New York.
- Marmont, G. 1949. Studies on the axon membrane. I. A new method. *J. Cell. Comp. Physiol.* 34:351-382.
- Maxwell, J. C. 1891. *A Treatise of Electricity and Magnetism*, Vols. I and II. Clarendon Press, Oxford, U.K.
- Miledi, R., I. Parker, and K. Sumikawa. 1983. Recording of single gamma-amino-butyrate- and acetylcholine-activated receptor channels translated by exogenous mRNA in *Xenopus* oocytes. *Proc. R. Soc. Lond. B.* 218:481-484.
- Peskoff, A., R. S. Eisenberg, and J. D. Cole. 1972. Potential induced by a point source of current in the interior of a spherical cell. UCLA-ENG-

- 7259, University of California, Los Angeles, School of Engineering and Applied Science.
- Peskoff, A., and R. S. Eisenberg. 1975. The time-dependent potential in a spherical cell using matched asymptotic expansions. *J. Math. Biol.* 2:277–300.
- Peskoff, A., and D. M. Ramirez. 1975. Potential induced in a spherical cell by an intracellular point source and an extracellular sink. *J. Math. Biol.* 2:301–316.
- Rall, W. 1953. Electrotonic theory for a spherical neurone. *Proc. Univ. Otago Med. School.* 31:14.
- Schreibmayer, W., H. A. Lester, and N. Dascal. 1994. Voltage clamping of *Xenopus laevis* oocytes utilizing agarose-cushion electrodes. *Pflügers Arch.* 426:453–458.
- Soreq, H., and S. Seidman. 1992. *Xenopus* oocyte microinjection: from gene to protein. In *Methods in Enzymology*. B. Rudy and L. E. Iverson, editors. Academic Press, San Diego. 207:225–265.
- Stümer, W., and A. B. Parekh. 1995. Electrophysiological recordings from *Xenopus* oocytes. In *Single-Channel Recording*. B. Sakmann and E. Neher, editors. Plenum Press, New York. 341–356.
- Tagliatalata, M., L. Toro, and E. Stefani. 1992. Novel voltage clamp to record small, fast currents from ion channels expressed in *Xenopus* oocytes. *Biophys. J.* 61:78–82.